

# Linear Temporal Logic Motion Planning for Teams of Underactuated Robots Using Satisfiability Modulo Convex Programming

Yasser Shoukry<sup>1</sup> Pierluigi Nuzzo<sup>2</sup> Ayca Balkan<sup>3</sup> Indranil Saha<sup>4</sup>  
Alberto L. Sangiovanni-Vincentelli<sup>5</sup> Sanjit A. Seshia<sup>5</sup> George J. Pappas<sup>6</sup> Paulo Tabuada<sup>3</sup>

**Abstract**—We present an efficient algorithm for multi-robot motion planning from linear temporal logic (LTL) specifications. We assume that the dynamics of each robot can be described by a discrete-time, linear system together with constraints on the control inputs and state variables. Given an LTL formula  $\psi$ , specifying the multi-robot mission, our goal is to construct a set of collision-free trajectories for all robots, and the associated control strategies, to satisfy  $\psi$ . We show that the motion planning problem can be formulated as the feasibility problem for a formula  $\varphi$  over Boolean and convex constraints, respectively capturing the LTL specification and the robot dynamics. We then adopt a satisfiability modulo convex (SMC) programming approach that exploits a monotonicity property of  $\varphi$  to decompose the problem into smaller subproblems. Simulation results show that our algorithm is more than one order of magnitude faster than state-of-the-art sampling-based techniques for high-dimensional state spaces while supporting complex missions.

## I. INTRODUCTION

An increasing number of safety-critical robotics applications (e.g., in rescue missions) as well as autonomous systems (e.g., unmanned aircraft and self-driving cars) require efficient techniques that can reason about hybrid system behaviors and guarantee the correctness of a controller implementation. Control synthesis from specifications captured by a logic formalism, such as linear temporal logic (LTL) [1], holds considerable promise for providing correct-by-construction implementations for a rich set of tasks [2]–[7]. However, the complexity of today’s robotics and autonomous systems poses several challenges to synthesis techniques.

A major difficulty stems from the need to reason about the tight integration of discrete abstractions (*task planning*) with continuous trajectories (*motion planning*) [8]. This integration can become daunting for high-dimensional systems, since a vast, discrete/continuous space must be searched while accounting for complex geometries, motion dynamics, collision avoidance, and temporal goals. In this paper, we address this challenge by focusing on the problem of *multi-robot motion planning* from LTL specifications. Given the robot model, a description of the workspace, and a task specification as an LTL formula  $\psi$ , we aim at planning collision-free and dynamically-feasible trajectories for all robots that satisfy  $\psi$ .

<sup>1</sup>Department of Electrical and Computer Engineering, University of Maryland, College Park, MD, <sup>2</sup>Department of Electrical Engineering, University of Southern California, Los Angeles, CA, <sup>3</sup>Department of Electrical Engineering, University of California, Los Angeles, CA, <sup>4</sup>Department of Computer Science and Engineering, Indian Institute of Technology, Kanpur, India, <sup>5</sup>Department of Electrical Engineering and Computer Sciences, University of California, Berkeley, CA, <sup>6</sup>Department of Electrical and Systems Engineering, University of Pennsylvania, Philadelphia, PA.

This work was partially sponsored by TerraSwarm, one of six centers of STARnet, a Semiconductor Research Corporation program sponsored by MARCO and DARPA, by the NSF project ExCAPE: Expeditions in Computer Augmented Program Engineering, and by NSF award 1239085.

While a growing body of work has focused, over the years, on the synthesis of reactive controllers that satisfy LTL specifications, a set of computational difficulties in this context still comes from the interplay between motion trajectories and task constraints. A first category of techniques for LTL motion planning utilizes a discrete abstraction of the system, often obtained by expensive discretizations of the continuous state space into polytopes, and an automata-theoretic approach to synthesize the controller [2]–[4]. A second category of approaches attempts at synthesizing the high-level planner together with the associated low-level controller, by either leveraging mixed integer linear programming (MILP) encodings of LTL specifications [9], [10] or sampling-based methods [7], [11], [12]. MILP-based planners can leverage the empirical performance of state-of-the-art solvers to solve for both the discrete and continuous constraints at the same time; however, they still tend to be impractical when the problem size grows. On the other hand, sampling-based techniques tend to require large computation time for obstacle avoidance problems in the presence of narrow passages [13] and for underactuated systems, e.g., systems with a lower number of actuators than degrees of freedom, under dynamic, in addition to kinematic, constraints. Moreover, sampling-based techniques do not have, in general, control over the length of the generated trajectory.

In this paper, we propose an efficient method for the integration of task planning and robot motion planning from generic LTL specifications based on the coordination of Boolean satisfiability (SAT) solving and convex programming. We consider the case of robots with dynamics that can be modeled as a discrete-time linear system. We then build on our results [14], [15] on motion planning for a single robot under reach-avoid specifications and extend our previous formulation to address, for the first time, multi-robot scenarios, including collision avoidance constraints, and arbitrary LTL specifications. We show that multi-robot motion planning can be formulated as the feasibility problem for a type of formula  $\varphi$ , called monotone satisfiability modulo convex formula, over a combination of Boolean and convex constraints, respectively capturing the LTL specification and the robot dynamics. We then adopt a *satisfiability modulo convex programming (SMC)* approach [15], [16] that exploits the monotonicity property of  $\varphi$  to decompose the problem into smaller subproblems that can be efficiently solved. Finally, we provide extensive comparisons of our approach with state-of-the-art sampling-based techniques, showing that our algorithm can run faster for high-dimensional state spaces.

## II. PROBLEM FORMULATION

We consider a set  $R$  of  $N$  robots that move in a workspace  $\mathcal{W} \subset \mathbb{R}^w$  where  $w$  can be 2 or 3, corresponding, respectively, to a 2-dimensional or 3-dimensional workspace. We use  $\|a\|$  to denote the infinity norm of  $a$ . We focus on the

centralized motion planning problem, without inter-robot communication, which we formulate as follows.

### A. Robot Model

We assume that the dynamics of robot  $R_i, i \in \{1, \dots, N\}$ , is described by a discrete-time linear system of the form:

$$\begin{aligned} x_{t+1}^i &= A_i x_t^i + B_i u_t^i, & (\text{II.1}) \\ x_0^i &= \bar{x}_0^i, \quad \|x_t^i\| \leq \bar{x}_i, \quad \|u_t^i\| \leq \bar{u}_i, \quad \forall t \in \mathbb{N} & (\text{II.2}) \end{aligned}$$

where  $x_t^i \in \mathcal{X} \subseteq \mathbb{R}^n$  is the state of robot  $R_i$  at time  $t \in \mathbb{N}$ ,  $u_t^i \in \mathcal{U} \subseteq \mathbb{R}^m$  is the robot input,  $\bar{x}_0^i$  is the robot initial state, and  $\bar{u}_i$  and  $\bar{x}_i$  are bounds on the input and state variables. The matrices  $A_i$  and  $B_i$  represent the robot dynamics and have appropriate dimensions. For a robot with nonlinear dynamics that is either differentially flat or feedback linearizable, the state space model (II.1) corresponds to its feedback linearized dynamics.

### B. Workspace

We assume that the robots must avoid a set of *obstacles*  $\mathcal{O} = \{\mathcal{O}_1, \dots, \mathcal{O}_o\}$ , with  $\mathcal{O}_i \subset \mathbb{R}^w$ , and represent the obstacle-free *workspace* as  $\mathcal{W} = \bigcup_1^r \mathcal{W}_i$ , where  $\bar{\mathcal{W}} = \{\mathcal{W}_1, \dots, \mathcal{W}_r\}$  is a set of non-overlapping *regions*, with  $\mathcal{W}_i \subset \mathbb{R}^w$ . Both the regions and the obstacles are assumed to be polygons.

For robot  $R_i$ , we can uniquely associate to each of the above regions a proposition in the set  $\Pi^i = \{\pi_1^i, \dots, \pi_r^i\}$ , where  $\pi_j^i$  evaluates to one (true) if robot  $R_i$  is in region  $\mathcal{W}_j$  and zero (false) otherwise. We then denote by  $h_{\mathcal{W} \rightarrow \Pi^i} : \mathcal{W} \rightarrow \Pi^i$  the map from each point  $w \in \mathcal{W}$  to the proposition  $\pi_j^i \in \Pi^i$  that evaluates to one at  $w$  for robot  $R_i$ . Moreover, a subset of each robot state variables, describing its position (coordinates), is also used to describe  $\mathcal{W}$ . Therefore, we denote as  $h_{\mathcal{X} \rightarrow \mathcal{W}} : \mathcal{X} \rightarrow \mathcal{W}$  the natural projection of the state  $x^i$  onto the workspace  $\mathcal{W}$ , and by  $h_{\mathcal{X} \rightarrow \Pi^i}$  the map from the state space of robot  $R_i$  to the set of propositions  $\Pi^i$ , obtained after projecting the state onto the workspace, i.e.,  $h_{\mathcal{X} \rightarrow \Pi^i}(x^i) = h_{\mathcal{W} \rightarrow \Pi^i}(h_{\mathcal{X} \rightarrow \mathcal{W}}(x^i))$ .

Finally, we introduce an *adjacency function*  $Adj : \bar{\mathcal{W}} \times \bar{\mathcal{W}} \rightarrow \mathbb{B}$  over the pairs of elements in  $\bar{\mathcal{W}}$  such that  $Adj(\mathcal{W}_i, \mathcal{W}_j) = 1$  if  $\mathcal{W}_i$  and  $\mathcal{W}_j$  are adjacent and 0 otherwise<sup>1</sup>. Because of the one-to-one correspondence between elements in  $\bar{\mathcal{W}}$  and propositions in  $\Pi^i$ , we also write  $Adj(\pi_j^i, \pi_k^i) = 1$  if  $\pi_j^i$  and  $\pi_k^i$  are associated with adjacent regions in  $\bar{\mathcal{W}}$  and 0 otherwise. Moreover, for all  $i$  and  $j$ ,  $Adj(\pi_j^i, \pi_j^i) = 1$  holds.

### C. Collision Avoidance

We require the distance (with respect to the infinity norm) between any two robots in the workspace at each time to be larger than an arbitrarily small positive number  $\epsilon \in \mathbb{R}^+$ . Formally,

$$\|h_{\mathcal{X} \rightarrow \mathcal{W}}(x_t^i) - h_{\mathcal{X} \rightarrow \mathcal{W}}(x_t^j)\| \geq \epsilon, \quad \forall t \geq 0, \quad (\text{II.3}) \\ \forall i, j \in \{1, \dots, N\}, i \neq j.$$

<sup>1</sup>Two polyhedra in  $\mathbb{R}^w$  are adjacent if they share a face of dimension  $w - 1$ .

### D. Linear Temporal Logic

We express the specification for a multi-robot mission using linear temporal logic (LTL) [1]. Let  $\Pi = \bigcup_{i=1}^R \Pi^i$  be the set of propositions associated with the workspace regions for all robots, as defined above. We consider formulas over a set of atomic propositions  $\Sigma$ , where  $\sigma(\pi) \in \Sigma$  is a Boolean or pseudo-Boolean predicate on  $\Pi$ . For example, we can express that ‘‘either robot  $R_1$  or  $R_2$  must be in  $\mathcal{W}_1$ ’’ via the proposition  $\sigma_1 := \pi_1^1 \vee \pi_1^2$  or that ‘‘at least one robot must be in  $\mathcal{W}_2$ ’’ using the proposition  $\sigma_2 := \sum_{i=1}^N \pi_2^i \geq 1$ .

From atomic propositions  $\sigma \in \Sigma$ , any LTL formula can be generated according to the following grammar:

$$\psi := \sigma \mid \neg\psi_0 \mid \psi_1 \wedge \psi_2 \mid \psi_1 \vee \psi_2 \mid \bigcirc\psi_0 \mid \psi_1 \mathcal{U} \psi_2 \mid \psi_1 \mathcal{R} \psi_2,$$

where  $\psi_0, \psi_1, \psi_2$  are LTL formulas. Given the above grammar, we can define *false* and *true* such that *false* =  $\psi \wedge \neg\psi$  and *true* =  $\neg\text{false}$ . Given the temporal operators *next* ( $\bigcirc$ ), *until* ( $\mathcal{U}$ ), and *release* ( $\mathcal{R}$ ), we can derive additional temporal operators, for example, *eventually* ( $\diamond$ ) and *always* ( $\square$ ), i.e.,  $\diamond\psi = \text{true} \mathcal{U} \psi$ , and  $\square\psi = \text{false} \mathcal{R} \psi$ . We refer the reader to the literature (e.g., [17]) for the formal semantics of LTL.

### E. Problem Definition

*Definition 2.1 (Problem Instance):* A problem instance is a tuple  $\mathcal{P} = (R, \mathcal{W}, \Pi, Adj, \Sigma, D, \bar{x}_0, \bar{x}, \bar{u}, \epsilon, \psi)$ , where:

- $R$  is the set of robots,
- $\mathcal{W}$  is the workspace,
- $\Pi$  is the set of propositions corresponding to the workspace regions and robots,
- $Adj$  is the adjacency function defining the connectivity of the different regions in the workspace,
- $\Sigma$  is the set of atomic propositions for the robot mission,
- $D = \{(A_1, B_1), \dots, (A_N, B_N)\}$  is the set of dynamics for the group of robots,
- $\bar{x}_0 = (\bar{x}_0^1, \dots, \bar{x}_0^N)$  is the set of initial states for the group of robots,
- $\bar{x} = (\bar{x}^1, \dots, \bar{x}^N)$  is the set of bounds on the states for the group of robot,
- $\bar{u} = (\bar{u}^1, \dots, \bar{u}^N)$  is the set of bounds on the control inputs for the group of robots,
- $\epsilon \in \mathbb{R}^+$  is the positive margin for collision avoidance,
- $\psi$  denotes the LTL specification defined over the atomic propositions  $\Sigma$  that the robots have to satisfy.

*Definition 2.2 (Trajectory):* A system *trajectory* for a problem instance  $\mathcal{P} = (R, \mathcal{W}, \Pi, Adj, \Sigma, D, \bar{x}_0, \bar{x}, \bar{u}, \epsilon, \psi)$  is a triple  $(x, \lambda, \rho(\lambda))$  including the following infinite sequences:

- $x = x_0 x_1 x_2 \dots$  is a sequence of system states, where the system state  $x_t = (x_t^1, \dots, x_t^N) \in \mathcal{X}^N$  includes the states of all the robots at time  $t$ ;
- $\lambda = \lambda_0 \lambda_1 \lambda_2 \dots$  is a sequence of valuations over  $\Pi$ , where  $\lambda_t = (\lambda_t^1, \dots, \lambda_t^N) \in \Pi^1 \times \dots \times \Pi^N$  is the set of workspace propositions that are true at  $x_t$ , i.e.,  $\lambda_t^i = h_{\mathcal{X} \rightarrow \Pi^i}(x_t^i)$  for all  $t \geq 0$  and  $i \in \{1, \dots, N\}$ ;
- $\rho(\lambda) = \rho_0(\lambda_0) \rho_1(\lambda_1) \rho_2(\lambda_2) \dots$  is a sequence of valuations over  $\Sigma$ , where  $\rho_t(\lambda_t)$  is the truth assignment associated with state  $x_t$  and propositions  $\lambda_t$ .

We call  $x$  and  $\lambda$ , respectively, the *state trajectory* and the *region trajectory* of the multi-robot system. Similarly, we call  $x^i = x_0^i x_1^i x_2^i \dots$  and  $\lambda^i = \lambda_0^i \lambda_1^i \lambda_2^i \dots$ , respectively, the state and region trajectory for robot  $R_i$ .

---

**Algorithm 1** SMC-BASED MOTION PLANNER

---

```
1: Initialize horizon:  $L := 1$ ;  
2: while Trajectory is not found do  
3:    $[[\mathcal{P}, L]]_D := \text{ENCODE-DIS-PLAN}(\mathcal{P}, L)$   
4:    $[[\mathcal{P}, L]]_C := \text{ENCODE-CON-PLAN}(\mathcal{P}, L)$   
5:    $(\text{STATUS}, \lambda, x, u) := \text{SMC.SOLVE}([[ \mathcal{P}, L ] ]_D, [[ \mathcal{P}, L ] ]_C)$ ;  
6:   if STATUS == UNSAT then  
7:     Increase horizon:  $L := L + 1$ ;  
8: return  $(\lambda, x, u)$ ;
```

---

*Definition 2.3 (Valid Trajectory):* A trajectory  $(x, \lambda, \rho)$  for a problem instance  $\mathcal{P} = \langle R, \mathcal{W}, \Pi, \text{Adj}, \Sigma, D, \bar{x}_0, \bar{x}, \bar{u}, \epsilon, \psi \rangle$  is a *valid trajectory* if the following holds:

- **Initial state constraint:**  $x_0 = \bar{x}_0$ ,
- **Dynamics, input, and state constraints:** for all  $i \in \{1, \dots, N\}$  and  $k \geq 0$  there exists  $u_k^i$  such that  $x_{k+1}^i = A_i x_k^i + B_i u_k^i$ ,  $\|x_k^i\| \leq \bar{x}^i$ , and  $\|u_k^i\| \leq \bar{u}^i$ ,
- **Workspace and obstacle avoidance constraints:**  $\text{Adj}(\lambda_k^i, \lambda_{k+1}^i) = 1$ ,  $\forall k \geq 0, \forall i \in \{1, \dots, N\}$ ,
- **Collision avoidance constraints:**  $\forall k \geq 0, \forall i, j \in \{1, \dots, N\}, i \neq j$ ,  $\|h_{\mathcal{X} \rightarrow \mathcal{W}}(x_k^i) - h_{\mathcal{X} \rightarrow \mathcal{W}}(x_k^j)\| \geq \epsilon$ ,
- **LTL constraints:**  $\rho$  satisfies the formula  $\psi$ , i.e.,  $\rho, 0 \models \psi$ .

We now formally define the motion planning problem that we solve in this paper.

*Problem 2.4 (Motion Planning Problem):* Given a problem instance  $\mathcal{P} = \langle R, \mathcal{W}, \Pi, \text{Adj}, \Sigma, D, \bar{x}_0, \bar{x}, \bar{u}, \epsilon, \psi \rangle$ , synthesize a valid trajectory for the multi-robot system.

### III. SMC-BASED SOLUTION STRATEGY

Using state space discretizations to account for constraints on the continuous dynamics may lead to state explosion as the number of continuous states and the number of obstacles increase. Our strategy aims, instead, at exploiting coarser abstractions of both the state space and the workspace, thus effectively decoupling the problem of *generating an obstacle-free path* from the ones of *checking physical realizability and collision avoidance*. By leveraging a satisfiability modulo convex (SMC) programming approach, we then partition the planning problem into two smaller subproblems involving reasoning, respectively, on sets of discrete and continuous variables from the original problem. These subproblems can be efficiently solved using specialized techniques.

As summarized in Algorithm 1, we first observe that the multi-robot motion planning problem for a fixed horizon  $L$  can be formulated as the feasibility problem for a special type of formula  $\varphi$  over Boolean and convex constraints, respectively capturing the constraints in the LTL specification  $\psi$  (subformula  $[[\mathcal{P}, L]]_D$ ) and the dynamics (subformula  $[[\mathcal{P}, L]]_C$ ). The formula  $\varphi$  is a monotone SMC formula that can be solved via a finite number of convex programs [15]. Specifically, SMC.SOLVE follows an iterative approach combining efficient SAT solving with a convex programming engine. At each iteration, the SAT solver generates candidate high-level paths  $\lambda$  that satisfy the set of constraints expressed by  $\psi$ . These paths are only defined over the set of Boolean propositions  $\Pi$  and ignore the robots' dynamics, input and state constraints, as well as the collision avoidance constraints.

The feasibility of the generated paths  $\lambda$  is then checked with respect to the system dynamics  $D$ , the control input bounds  $\bar{u}$ , the state bounds  $\bar{x}$ , the robots' initial states  $\bar{x}_0$ ,

and the collision avoidance constraints, by casting a convex optimization problem. If both the Boolean and the real-valued constraints are satisfied, a valid trajectory is returned, consisting of the proposed plan and the corresponding state and control input trajectories for the group of robots. Otherwise, the proposed sequence  $\lambda$  is marked as infeasible and new candidate plans are generated until either a feasible one is found, or SMC.SOLVE returns UNSAT, meaning that no trajectory is feasible for the current horizon length.

Checking the feasibility of a set of convex constraints can be performed efficiently, with a complexity that is polynomial in the number of constraints and real variables. On the other hand, the worst case bound on the number of iterations between the SAT solving and convex programming routines in SMC.SOLVE is exponential in the number of convex constraints in  $\varphi$ . A prominent feature of SMC is, however, the generation of compact infeasibility certificates, i.e., “succinct explanations” that can capture the root causes for the infeasibility of a plan and rule out the largest possible number of invalid plans for the SAT solver to accelerate the search. In what follows, we provide details on the encodings of both the discrete and continuous planning problems and discuss the formal guarantees of Algorithm 1.

### IV. SMC ENCODING OF THE PROBLEM

#### A. Encoding the High-Level Discrete Planning Problem

We translate the high-level, discrete planning problem into a conjunction of Boolean constraints using the Bounded Model Checking (BMC) encoding technique for LTL model checking by Biere et al. [17]. Though a trace that satisfies an LTL formula is given as an infinite execution path of the system, such trace can be represented by a finite path under the following conditions: (i) the finite path is a valid prefix of all its infinite extensions, (ii) a portion of the finite path can loop to generate a valid infinite path. Let  $(x, \lambda, \rho(\lambda))$  be a valid trajectory of the system under generic LTL constraints. The system trajectory  $\rho = \rho_0 \rho_1 \rho_2 \dots$  can then be represented as:

$$\rho = (\rho_0 \rho_1 \dots \rho_{k-1}) (\rho_k \dots \rho_L)^\omega,$$

where  $0 < k \leq L$  and  $\rho_L = \rho_{k-1}$ . Such a representation of a trajectory is called an  $(L, k)$ -loop. The trajectory  $(\rho_k \dots \rho_L)^\omega$  denotes an infinite trajectory that can be obtained by repeating the sequence  $(\rho_k \dots \rho_L)$ .

Given a problem instance  $\mathcal{P} = \langle R, \mathcal{W}, \Pi, \text{Adj}, \Sigma, D, \bar{x}_0, \bar{x}, \bar{u}, \epsilon, \psi \rangle$ , and a positive constant  $L$ , let  $(\bar{x}_0, \bar{\lambda}_0)$  represent the initial state of the system, where  $\bar{x}_0 = (\bar{x}_0^1, \dots, \bar{x}_0^N)$ ,  $\bar{\lambda}_0 = (\bar{\lambda}_0^1, \dots, \bar{\lambda}_0^N)$  and, for all  $i \in \{1, \dots, N\}$ ,  $\bar{\lambda}_0^i = h_{\mathcal{X} \rightarrow \Pi^i}(\bar{x}_0^i)$ . Our objective is to generate a formula that represents any valid trajectory of the multi-robot system in the form of an  $(L, k)$ -loop. The decision variables for the formula are ultimately given by the propositions associated with the workspace regions to be occupied by each robot and the variable  $k$  represents the location at which the loop starts. Specifically, for all  $i \in \{1, \dots, N\}$ ,  $j \in \{1, \dots, r\}$ ,  $t \in \{0, \dots, L\}$ , we introduce a Boolean variable  $\pi_{jt}^i$  which evaluates to one if and only if robot  $R_i$  is in region  $\mathcal{W}_j$  at time  $t$ . Let  $\bar{\Pi}$  be the set of all these decision variables. Based on these variables, the encoding of the discrete trajectory synthesis problem is linear in  $L$  and captures three kinds of constraints:

- Workspace and obstacle avoidance constraints, denoted by  $[[\mathcal{W}]]$ ,
- LTL formula constraints, denoted by  $[[LTL]]$ ,

- Loop constraints, denoted by  $[[LOOP]]$ .

1) *Workspace Constraints*: A set of workspace constraints can be captured by the following formula:

$$[[\mathcal{W}]] := (\lambda_0 = \bar{\lambda}_0) \wedge \bigwedge_{i=1}^N \bigwedge_{t=1}^L \lambda_t^i \in \mathcal{N}(\lambda_{t-1}^i),$$

where  $\mathcal{N}(\lambda_t^i) = \{\pi_j^i \in \Pi^i \mid Adj(\lambda_t^i, \pi_j^i) = 1\}$  denotes the set of regions that are adjacent (neighbors) to  $\lambda_t^i$ . The above formula enforces that the trajectory starts with the initial regions in  $\bar{\lambda}_0$  and proceeds by only visiting regions that are adjacent. For instance, adjacency constraints can be encoded using the variables in  $\bar{\Pi}$  as follows:  $\forall i \in \{1, \dots, N\}, t \in \{1, \dots, L-1\}, j \in \{1, \dots, r\}$ ,

$$\pi_{j(t-1)}^i \Rightarrow \bigvee_{j' \in \mathcal{I}(j)} \pi_{j't}^i,$$

where  $\mathcal{I}(j) = \{j' \mid Adj(\pi_j^i, \pi_{j'}^i) = 1, \pi_{j'}^i \in \Pi^i\}$ . At each time  $t$  and for each robot  $R_i$  only one of the  $\pi_{j't}^i$  can be one, which can be captured by the following pseudo-Boolean constraints:

$$\sum_{j=1}^r \pi_{j't}^i = 1, \quad \forall i \in \{1, \dots, N\}, \quad \forall t \in \{0, \dots, L\},$$

which are also part of the formula  $[[\mathcal{W}]]$ . Obstacle avoidance is implicitly encoded by the fact that  $\bar{\Pi}$  and  $Adj$  are defined only over the regions in the free space.

2) *LTL and Loop Constraints*: We generate the Boolean constraints  $[[LTL]]$  and  $[[LOOP]]$ , capturing the LTL formula specification, using the *eventuality encoding* [17]. Specifically,  $[[LOOP]]$  ensures the preservation of the correct semantics of the  $\mathcal{U}$  operator when the generated trajectory contains a loop.

3) *Full Discrete Problem Encoding*: The full encoding of the discrete portion of the problem is denoted by  $[[\mathcal{P}, L]]_D$ , and is given by the conjunction of the above three sets of constraints and the constraint that ensures that the LTL formula  $\psi$  holds in the initial state:

$$[[\mathcal{P}, L]]_D \Leftrightarrow [[\mathcal{W}]] \wedge [[LTL]] \wedge [[LOOP]] \wedge b_0^{\psi}$$

## B. Encoding the Low-Level Motion Planning Problem

A valid trajectory must satisfy a set of dynamic, input, and state constraints, as well as collision avoidance constraints. We encode them via a conjunction of hybrid constraints including Boolean variables, as well as convex constraints on the reals.

**Dynamics, State, and Input Constraints.** We enforce that valid trajectories progress according to the robots' dynamics with the conjunction of the following constraints:

$$\begin{aligned} x_{t+1}^i &= A_i x_t^i + B_i u_t^i, & \forall t \in \{0, \dots, L-1\}, \forall i \in \{1, \dots, N\} \\ x_0^i &= \bar{x}_0^i, & \forall i \in \{1, \dots, N\} \\ \|x_t^i\| &\leq \bar{x}^i & \forall t \in \{0, \dots, L-1\}, \forall i \in \{1, \dots, N\} \\ \|u_t^i\| &\leq \bar{u}^i & \forall t \in \{0, \dots, L-1\}, \forall i \in \{1, \dots, N\} \end{aligned} \quad (\text{IV.1})$$

**Maintaining Consistency Between Regions and States.** The state of each robot must be consistent with the workspace region occupied at each time. Since each

workspace region  $\mathcal{W}_j$  is a polyhedron, it can be captured by an affine inequality of the form ( $P_j w + q_i \leq 0$ ). We therefore obtain,  $\forall i \in \{1, \dots, N\}$ :

$$\begin{aligned} \pi_{j't}^i &\Rightarrow (P_j h_{\mathcal{X} \rightarrow \mathcal{W}}(x_t^i) + q_j \leq 0), & \forall t \in \{0, \dots, L\}, \\ & & j \in \{1, \dots, r\} \\ l_t &\Rightarrow (x_L^i = x_{t-1}^i), & \forall t \in \{1, \dots, L\}, \end{aligned} \quad (\text{IV.2})$$

where  $h_{\mathcal{X} \rightarrow \mathcal{W}}(\cdot)$ , the natural projection of the state space onto the workspace, is also an affine function. We also require that, if there is a loop, the state of each robot at time  $L$  is identical to its state before the loop starts. While this is only a sufficient condition for the existence of a continuous trajectory that is consistent with the discrete plan, it can be shown from reachability analysis that this condition becomes necessary under some technical assumptions on the robot dynamics [18].

**Collision Avoidance Constraints.** For each pair of robots at each time and a workspace of dimension  $w$ , we create pairs of fresh Boolean variables  $\{(c_{kt}^{ij}, d_{kt}^{ij}) \mid t \in \{0, \dots, L\}, k \in \{1, \dots, w\}, i, j \in \{1, \dots, N\}, i \neq j\}$  and encode the collision avoidance conditions via the conjunction of the following constraints:

$$\begin{aligned} \forall i, j \in \{1, \dots, N\}, i \neq j, \forall t \in \{0, \dots, L\}: \\ c_{kt}^{ij} &\Rightarrow (h_{\mathcal{X} \rightarrow \mathcal{W}}^k(x_t^i) - h_{\mathcal{X} \rightarrow \mathcal{W}}^k(x_t^j)) \geq \epsilon, \forall k \in \{1, \dots, w\} \\ d_{kt}^{ij} &\Rightarrow (-h_{\mathcal{X} \rightarrow \mathcal{W}}^k(x_t^i) + h_{\mathcal{X} \rightarrow \mathcal{W}}^k(x_t^j)) \geq \epsilon, \forall k \in \{1, \dots, w\} \\ \sum_{k=1}^w (c_{kt}^{ij} + d_{kt}^{ij}) &\geq 1, \end{aligned} \quad (\text{IV.3})$$

where  $h_{\mathcal{X} \rightarrow \mathcal{W}}^k(\cdot)$  is the natural projection of the state space onto the  $k$ -th dimension of the workspace.

The conjunction of the sets of constraints (IV.1), (IV.2), and (IV.3), denoted as  $[[\mathcal{P}, L]]_C$ , is conjoined with the formula  $[[\mathcal{P}, L]]_D$  for the discrete plan to provide the overall formula  $[[\mathcal{P}, L]]$  encoding the motion planning problem in this paper:

$$[[\mathcal{P}, L]] \Leftrightarrow [[\mathcal{P}, L]]_D \wedge [[\mathcal{P}, L]]_C. \quad (\text{IV.4})$$

The following result states that  $[[\mathcal{P}, L]]$  can be efficiently solved by combining SAT solving, convex programming, and conflict-driven learning techniques, as shown in Algorithm 1, since it falls into the category of monotone SMC formulas.

*Proposition 4.1 (Monotone SMC-Based Encoding):*

Given a multi-robot motion planning problem instance  $\mathcal{P}$  and a finite horizon  $L$ , let  $[[\mathcal{P}, L]]$  be the formula obtained in (IV.4).  $[[\mathcal{P}, L]]$  is a monotone SMC formula, hence its satisfiability problem can be cast as the feasibility problem for a finite disjunction of convex programs, and solved as shown in Algorithm 1.

We can finally state the formal guarantees of Algorithm 1.

*Theorem 4.2 (Correctness of Algorithm 1):* Given a multi-robot motion planning problem instance  $\mathcal{P}$ , Algorithm 1, leveraging the SMC-based encoding  $[[\mathcal{P}, L]]$  in (IV.4), is sound.

## V. RESULTS

We implemented Algorithm 1 in PYTHON on top of the SATEX solver [15], using Z3 [19] as a SAT solver and CPLEX [20] as a convex optimization solver. We generate infeasibility certificates that are minimal by providing, at

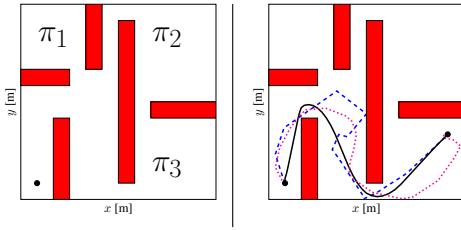


Fig. 1. (Left) Workspace and propositions used in our experiments; (right) trajectories generated by the SMC-based (black), Synergistic RRT (dashed blue), and Synergistic EST (dotted red) motion planners for the double integrator dynamics.

each iteration, an Irreducibly Inconsistent Set (IIS) of linear constraints [21]. Moreover, in each convex program, we instruct SATEX to search for a continuous trajectory that minimizes the  $\ell_1$ -norm of the overall control “effort”  $\sum_{0 \leq t \leq L, 1 \leq i \leq N} \|u_i^t\|_1$ , over all robots at all times, among the trajectories compatible with the discrete plan from the SAT solver. All the experiments were executed on an Intel Core i7 3.4-GHz processor with 16 GB of memory.

### A. Single-Robot Reach-Avoid Specification

As a first scenario to validate our approach, we consider a single robot subject to a reach-avoid specification, an essential motion planning problem, which is embedded in almost all robotics applications. A single-robot scenario also allows comparing against alternative sampling-based algorithms which do not support, as yet, multi-robot formulations. We consider the workspace represented on the left side of Figure 1, where the black dot marks the initial position of the robot. We compare the performance of our algorithm against state-of-the-art sampling-based techniques implemented in Syclop (Synergistic Combination of Layers Of Planning), which have been shown to outperform traditional sampling-based algorithms by orders of magnitude [22]. Syclop is available from the Open Motion Planning Library (OMPL)<sup>2</sup>. We consider two versions, namely, Syclop RRT (Rapidly-exploring Random Trees) and Syclop EST (Expansive Space Trees). We also compare with state-of-the-art SMT solvers supporting nonlinear constraints on the reals, namely, Z3 and DREAL [23], when directly applied to the monotone SMC formula encoding the motion planning problem. MILP-based techniques are not considered in this paper, since the SMC-based planner has already been shown to scale better on similar problems [14], [15].

We consider robot dynamics captured by chains of integrators, one chain for each coordinate of the workspace, and a sampling time of 0.5 s. The robot starts at the point with coordinates (0.5, 0.5) (in meters) and is required to reach the point (5.5, 2.0), while higher order derivatives are set to 0 both at the initial and target points. The corresponding LTL formula is  $\psi_1 := (\bigwedge_j \neg \eta_j) \mathcal{U} \gamma$ , where  $\eta_j$ ,  $j \in \{1, \dots, o\}$ , are propositions associated with the obstacles and  $\gamma$  is the proposition associated with the goal region in the workspace. The upper bound on the control input is  $\bar{u} = 0.2$ , in appropriate units based on the number of integrators in the chain. Table I reports the execution times of different algorithms as the number of integrators in the chain, hence the number of state variables, increases. Times are averaged over 20 trials. RRT and EST-based planners show much higher variability in execution time than the SMC-based planner, as is expected

<sup>2</sup><https://ompl.kavrakilab.org/planners.html>

TABLE I  
EXECUTION TIME OF DIFFERENT MOTION PLANNING ALGORITHMS AS A FUNCTION OF THE NUMBER OF CONTINUOUS STATES FOR THE WORKSPACE IN FIG. 1. RESULTS ARE AVERAGED ACROSS 20 TRIALS. TIMEOUT IS SET TO 1 HOUR.

Number of States	SMC-Based [s]	Synergistic RRT [s]	Synergistic EST [s]	dReal [s]	Z3 [s]
4	3.007	33.166	0.6151	timeout	timeout
6	4.590	3216.402	791.444	timeout	timeout
8	7.502	timeout	timeout	timeout	timeout
10	10.207	timeout	timeout	timeout	timeout
12	34.775	timeout	timeout	timeout	timeout
14	60.413	timeout	timeout	timeout	timeout
16	39.070	timeout	timeout	timeout	timeout
18	70.631	timeout	timeout	timeout	timeout
20	75.843	timeout	timeout	timeout	timeout

TABLE II  
EXECUTION TIME OF THE SMC-BASED MOTION PLANNER VERSUS SYCLOP LTL. TIMEOUT IS SET TO 15 MINUTES.

Number of States	Number of Propositions	SMC-Based [s]	Synergistic LTL [s]
4	1	6.6614	2.4978
	2	16.0456	44.3815
	3	36.651	153.389
6	1	25.2670	13.003
	2	54.517	timeout
	3	73.0913	timeout
8	1	6.280	timeout
	2	26.385	timeout
	3	225.255	timeout

because of their randomized search schemes. Syclop EST performs better for a small number of continuous states, but its runtime rapidly increases and reaches a 1-hour timeout for a chain of four integrators. Our algorithm scales better over the whole range of continuous states scoring more than one order of magnitude reduction in computation time. Moreover, the generated trajectory is usually smoother because of the  $\ell_1$ -norm minimization. Z3 and DREAL exceed the timeout threshold in all the experiments.

### B. Single Robot Under LTL Specifications

While our encoding supports generic LTL specifications, in this scenario, we only focus on co-safe LTL formulas, since this is the only fragment supported by the Syclop LTL motion planner version. We consider the same workspace and initial condition as in Figure 1 under LTL formulas of the form  $\psi_2 := \bigwedge_i \diamond \pi_i \bigwedge_j \square \neg \eta_j$ , where  $\eta_j$ ,  $j \in \{1, \dots, o\}$ , are propositions associated with the obstacles in the workspace. The robot must visit a set of regions, in arbitrary order, while avoiding obstacles.

Table II reports the execution times of our algorithm and Syclop LTL as both the number of chained integrators capturing the robot dynamics, hence the number of continuous variables, and the number of regions to be visited, hence the number of Boolean variables in the specification, increase. Results are averaged over 10 trials. Syclop exceeds the 15-minute timeout threshold for a system with 3 integrators and an LTL specification including two regions ( $i=2$ ). In the case of one region to be visited for a 3-integrator chain, Syclop reaches the timeout value in 4 runs; we then report the average time over the remaining 6 runs.

### C. Multi-Robot Scenarios

We first show the effectiveness of the proposed collision avoidance encoding on the workspace in Figure 2, where we force the robots to “cross” each other in the same region as they move from their initial positions to their targets subject to reach-avoid specifications. Table III reports the

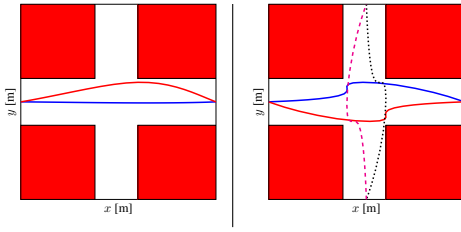


Fig. 2. Workspace and trajectories under reach avoid specifications for a 2-robot scenario (left) and a 4-robot scenario (right).

TABLE III

PERFORMANCE OF THE SMC-BASED MOTION PLANNER AND SIZE OF THE PROBLEM IN MULTI-ROBOT SCENARIOS WITH REACH-AVOID SPECIFICATION AND SPECIFICATION  $\psi_3$ .

Number of Robots	Number of States (per robot)	SMC-Based Reach-avoid specification			SMC-Based $\psi_3 := (\Box\Diamond\sigma_1) \wedge (\Box\Diamond\sigma_2) \wedge (\Box\Diamond\sigma_3)$		
		time [s]	#real vars	#Boolean vars	time [s]	#real vars	#Boolean vars
2	4	0.3346	336	66	19.269	960	2370
	6	0.822	420		44.72625	1200	
	8	1.0625	504		67.6701	1440	
	10	0.915	588		76.3877	1680	
3	12	2.444	672	117	665.4057	1920	3449
	4	0.7170	504		105.661	1440	
	6	2.1074	630		196.425	1800	
	8	3.8263	756		253.077	2160	
4	10	15.005	882	180	1151.087	2520	4648
	12	8.654	1008		466.6257	2880	
	4	0.9621	672		444.354	1920	
	6	5.1138	840		829.665	2400	
5	8	6.3493	1008	255	986.9366	2880	5967
	10	44.4658	1176		timeout	3360	
	12	80.0632	1344		timeout	3840	
	4	5.8121	840		1334.822	2400	
6	4	26.4051	1008	342	timeout	2880	7406
7	4	142.896	1008	441	timeout	3360	8965
8	4	1229.5425	1344	552	timeout	3840	10644

performance of our motion planner as the number of robots (hence the number of Boolean variables in the problem) and the number of integrators (hence the continuous states in the problem) increase. Trajectories for a 2-robot and a 4-robot scenario are visualized, respectively, on the left and right sides of Figure 2, illustrating the satisfaction of the collision avoidance constraints with a safety margin  $\epsilon = 0.2$  m.

We finally demonstrate the capabilities of our algorithm in a multi-robot scenario under generic LTL specifications. We consider the workspace in Figure 1, an even number of robots  $N$ , and the LTL formula  $\psi_3 := (\Box\Diamond\sigma_1) \wedge (\Box\Diamond\sigma_2) \wedge (\Box\Diamond\sigma_3)$ , where  $\sigma_1 := \sum_{i=1}^N \pi_1^i = N$ ,  $\sigma_2 := \sum_{i=1}^{N/2} \pi_2^i = N/2$ , and

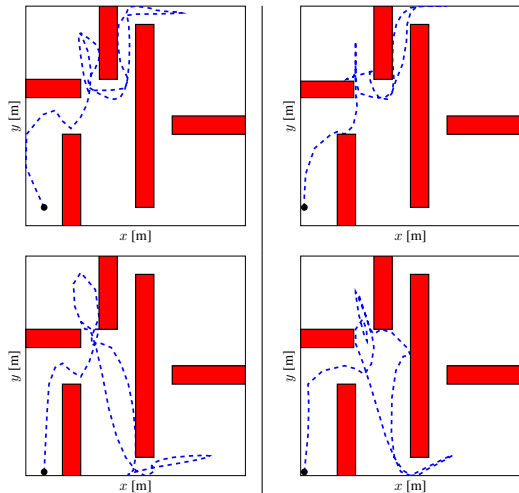


Fig. 3. Trajectories of robots  $R_1$ ,  $R_2$ ,  $R_3$ , and  $R_4$  (from left to right), subject to  $\psi_3 := (\Box\Diamond \sum_{i=1}^4 \pi_1^i = 4) \wedge (\Box\Diamond \sum_{i=1}^2 \pi_2^i = 2) \wedge (\Box\Diamond \sum_{i=3}^4 \pi_3^i = 2)$ . The trajectories of  $R_1$  and  $R_2$  visit region 2 while the ones of  $R_3$  and  $R_4$  touch region 3 as specified.

$\sigma_3 := \sum_{i=N/2+1}^N \pi_3^i = N/2$ . In words, we require the robots to visit, all together, region 1 infinitely often. Similarly, a first half of robots must also visit region 2, while the second half must visit region 3, all together, infinitely often. Again, we report in Table III the performance of our motion planner as the number of robots and chained integrators increase together with the problem size in terms of number of Boolean and real variables. The trajectories for the 4-robot scenario are separately shown in Figure 3.

## REFERENCES

- [1] A. Pnueli, "The temporal logic of programs," in *FOCS*, 1977, pp. 46–57.
- [2] P. Tabuada and G. J. Pappas, "Linear time logic control of discrete-time linear systems," *IEEE Trans. Automatic Control*, vol. 51, no. 12, pp. 1862–1877, 2006.
- [3] G. E. Fainekos, A. Girard, H. Kress-Gazit, and G. J. Pappas, "Temporal logic motion planning for dynamic robots," *Automatica*, vol. 45, no. 2, pp. 343–352, 2009.
- [4] T. Wongpiromsarn, U. Topcu, and R. M. Murray, "Receding horizon temporal logic planning," *IEEE Trans. Automatic Control*, vol. 57, no. 11, pp. 2817–2830, 2012.
- [5] P. Nuzzo, H. Xu, N. Ozay, J. Finn, A. Sangiovanni-Vincentelli, R. Murray, A. Donze, and S. Seshia, "A contract-based methodology for aircraft electric power system design," *IEEE Access*, vol. 2, pp. 1–25, 2014.
- [6] I. Saha, R. Ramaithitima, V. Kumar, G. J. Pappas, and S. A. Seshia, "Automated composition of motion primitives for multi-robot systems from safe LTL specifications," in *Int. Conf. Intelligent Robots and Systems*, 2014, pp. 1525–1532.
- [7] C. I. Vasile and C. Belta, "Sampling-based temporal logic path planning," in *Intelligent Robots and Systems (IROS), 2013 IEEE/RSJ International Conference on*. IEEE, 2013, pp. 4817–4822.
- [8] E. Plaku and S. Karaman, "Motion planning with temporal-logic specifications: Progress and challenges," *AI Communications*, vol. 29, no. 1, pp. 151–162, 2016.
- [9] S. Karaman and E. Frazzoli, "Linear temporal logic vehicle routing with applications to multi-UAV mission planning," *Int. J. Robot and Nonlinear Control*, vol. 21, no. 12, pp. 1372–1395, 2011.
- [10] E. M. Wolff, U. Topcu, and R. M. Murray, "Optimization-based trajectory generation with linear temporal logic specifications," in *IEEE Int. Conf. Robotics and Automation*, 2014, pp. 5319–5325.
- [11] S. Karaman and E. Frazzoli, "Sampling-based motion planning with deterministic  $\mu$ -calculus specifications," in *Proc. IEEE Conf. Decision and Control*, 2009, pp. 2222–2229.
- [12] A. Bhatia, L. E. Kavraki, and M. Y. Vardi, "Sampling-based motion planning with temporal goals," in *IEEE Int. Conf. Robotics and Automation*, 2010, pp. 2689–2696.
- [13] L. Zhang and D. Manocha, "An efficient retraction-based RRT planner," in *IEEE Int. Conf. Robotics and Automation*, 2008, pp. 3743–3750.
- [14] Y. Shoukry, P. Nuzzo, I. Saha, A. Sangiovanni-Vincentelli, S. Seshia, G. Pappas, and P. Tabuada, "Scalable lazy SMT-based motion planning," in *Proc. IEEE Conf. Decision and Control*, 2016, pp. 6683–6688.
- [15] Y. Shoukry, P. Nuzzo, A. Sangiovanni-Vincentelli, S. A. Seshia, G. J. Pappas, and P. Tabuada, "SMC: Satisfiability modulo convex optimization," in *Proc. Int. Conf. Hybrid Systems: Computation and Control*, Apr. 2017.
- [16] P. Nuzzo, A. Puggelli, S. A. Seshia, and A. Sangiovanni-Vincentelli, "CalCS: SMT solving for non-linear convex constraints," in *Int. Conf. Formal Methods in Computer-Aided Design*, Oct. 2010, pp. 71–79.
- [17] A. Biere, K. Heljanko, T. Junttila, T. latvala, and V. Schuppan, "Linear encoding of bounded LTL model checking," *Logical Methods in Computer Science*, vol. 2, no. 5:5, pp. 1–64, 2006.
- [18] P. Tabuada, *Verification and control of hybrid systems: a symbolic approach*. Springer Science & Business Media, 2009.
- [19] L. De Moura and N. Björner, "Z3: An efficient SMT solver," in *Proc. Int. Conf. Tools and Algorithms for the Construction and Analysis of Systems*, 2008, pp. 337–340.
- [20] (2012, Feb.) IBM ILOG CPLEX Optimizer. [Online]. Available: [www.ibm.com/software/integration/optimization/cplex-optimizer/](http://www.ibm.com/software/integration/optimization/cplex-optimizer/)
- [21] J. W. Chinneck and E. W. Dravnieks, "Locating minimal infeasible constraint sets in linear programs," *ORSA Journal on Computing*, vol. 3, no. 2, pp. 157–168, 1991.
- [22] E. Plaku, L. E. Kavraki, and M. Y. Vardi, "Motion planning with dynamics by a synergistic combination of layers of planning," *IEEE Transactions on Robotics*, vol. 26, no. 3, pp. 469–482, Jun. 2010.
- [23] S. Gao, S. Kong, and E. M. Clarke, "dReal: An SMT solver for nonlinear theories over the reals," in *Int. Conf. Automated Deduction*, 2013, vol. 7898, pp. 208–214.